
De novo design of antibody heavy chains with SE(3) diffusion

Anonymous Author(s)

Affiliation
Address
email

Abstract

1 We introduce *VH-Diff*, an antibody heavy chain variable domain diffusion model.
2 This model is based on *FrameDiff*, a general protein backbone diffusion framework,
3 which was fine-tuned on antibody structures. The backbone dihedral angles of
4 sampled structures show good agreement with a reference antibody distribution. We
5 use an antibody-specific inverse folding model to recover sequences corresponding
6 to the predicted structures, and study their validity with an antibody numbering
7 tool. Assessing the designability and novelty of the structures generated with our
8 heavy chain model we find that *VH-Diff* produces highly designable structures that
9 can contain novel binding regions. Finally, we compare our model with a state-of-
10 the-art sequence-based generative model and show more consistent preservation of
11 the conserved framework region with our structure-based method.

12 1 Introduction

13 Engineering novel proteins that can satisfy specified functional properties is the central aim of rational
14 protein design. While sequence-based methods have seen some success [Wu et al., 2021], they are
15 intrinsically limited by the fact that most properties of a molecule, such as binding or solubility, are
16 determined by their three-dimensional structure. Recent advances in diffusion models [Ho et al.,
17 2020, Song et al., 2021], a class of deep probabilistic generative models, have shown promise as a
18 data-driven alternative to more computationally expensive physics-based methods [Alford et al., 2017]
19 in tackling *de novo* protein design. Most approaches focus on modelling only the backbone [Watson
20 et al., 2022, Lin and AlQuraishi, 2023], while the sequence is inferred through an inverse folding
21 model, though some full-atom models have been explored [Chu et al., 2023, Martinkus et al., 2023].

22 An application of particular therapeutic relevance is the design of immunoglobulin proteins, which
23 play a central role in helping the adaptive immune system identify and neutralise pathogens. They
24 consist of two heavy and two light chains. These are separated into constant domains that specify
25 effector function, and a variable domain that contains six hypervariable loops, known as the comple-
26 mentarity determining regions (CDR), which control binding specificity. Monoclonal antibodies are
27 an emerging drug modality with the potential for applications in a wide range of therapeutic areas, for
28 example onconogenic, infectious and autoimmune diseases. They can be adapted to target specific
29 antigens or receptors through engineering of the binding site [Chiu et al., 2019].

30 In this article, we consider the recent backbone diffusion model *FrameDiff* [Yim et al., 2023] and
31 fine-tune it on synthetic antibody structures from the ImmuneBuilder dataset [Abanades et al., 2022].
32 We focus on the variable region of the heavy chain, which is the most structurally diverse domain
33 of the antibody, and whose CDR-H3 often determines antigen recognition [Narciso et al., 2011,
34 Tsuchiya and Mizuguchi, 2016]. We study the designability and novelty of the structures generated

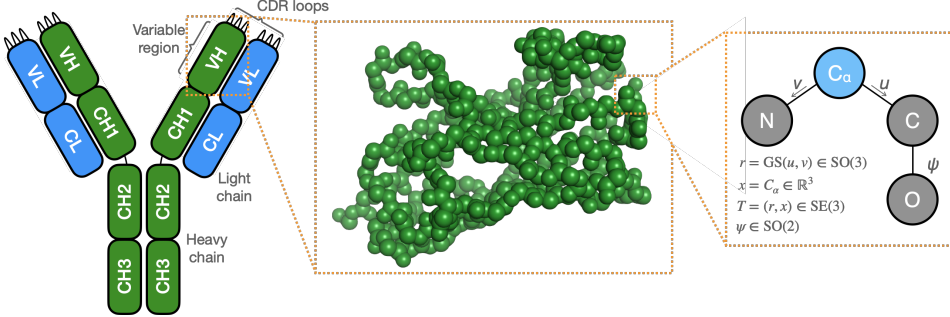


Figure 1: Schematic representation of an antibody, the heavy chain variable domain, and the parametrisation of backbone residues into frames used by the diffusion model. Each frame consists of four heavy atoms connected by rigid covalent bonds.

35 by our heavy chain model and predict the corresponding sequences with AbMPNN [Dreyer et al.,
 36 2023], an antibody-specific inverse folding model based on ProteinMPNN [Dauparas et al., 2022].

37 2 SE(3) protein backbone diffusion model

38 We review the SE(3) diffusion framework introduced in Yim et al. [2023], which constructs an explicit
 39 framework for the diffusion of protein backbones based on the Riemannian score-based generative
 40 modeling approach of Bortoli et al. [2022].

41 For the backbone frame parametrisation we adopt the same formalism as in AlphaFold2 [Jumper
 42 et al., 2021], using a collection of N orientation preserving rigid transformations to represent an N
 43 residue backbone, as shown in figure 1. These frames map from fixed coordinates of the four heavy
 44 atoms $N^*, C_\alpha^*, C^*, O^* \in \mathbb{R}^3$ centered at $C_\alpha^* = \vec{0}$, assuming experimentally measured bond lengths
 45 and angles [Engh and Huber, 2012]. The main backbone atomic coordinates for a residue i are given
 46 through

$$[N_i, C_i, C_{\alpha,i}] = T_i \cdot [N^*, C^*, C_\alpha^*], \quad (1)$$

47 where $T_i \in \text{SE}(3)$ is a member of the special Euclidean group, the set of valid translations and
 48 rotations in Euclidean space. A backbone consists of N frames $[T_1, \dots, T_N] \in \text{SE}(3)^N$, with the
 49 oxygen atom O being reconstructed from an additional torsion angle $\psi \in \text{SO}(2)$ around the C_α and
 50 C bond. Each frame is decomposed into $T_i = (r_i, x_i)$, where $x_i \in \mathbb{R}^3$ is the C_α translation and
 51 $r_i \in \text{SO}(3)$ is a 3×3 rotation matrix which can be derived from relative atom positions with the
 52 Gram-Schmidt process. A diffusion process over $\text{SE}(3)^N$ can be constructed to achieve global $\text{SE}(3)$
 53 invariance by keeping the diffusion process centered at the origin.

54 We model the distribution over $\text{SE}(3)^N$ through Riemannian score-based generative modeling, which
 55 aims to sample from a distribution supported on a Riemannian manifold \mathcal{M} by reversing a forward
 56 process that evolves from the data distribution p_0 towards an invariant density p_T through

$$d\mathbf{X}_t = -\frac{1}{2}\nabla U(\mathbf{X}_t)dt + d\mathbf{B}_{t,\mathcal{M}}, \quad \mathbf{X}_0 \sim p_0, \quad (2)$$

57 where $\mathbf{B}_{t,\mathcal{M}}$ is the Brownian motion on \mathcal{M} , $U(x)$ is a continuously differentiable variable defining
 58 the invariant density $p_T \propto e^{-U(x)}$, ∇ is the Riemannian gradient, and $t \in [0, T]$ is a continuous time
 59 variable. The time-reversed process for $\mathbf{Y}_t = \mathbf{X}_{T-t}$ also satisfies a stochastic differential equation
 60 given by

$$d\mathbf{Y}_t = [\frac{1}{2}\nabla U(\mathbf{Y}_t) + \nabla \log p_{T-t}(\mathbf{Y}_t)]dt + d\mathbf{B}_{t,\mathcal{M}}, \quad \mathbf{Y}_0 \sim p_T, \quad (3)$$

61 where p_t is the density of \mathbf{X}_t . The Riemannian gradients and Brownian motion depend on a choice
 62 of inner product on \mathcal{M} , which for $\text{SE}(3)$ can simply be derived from the canonical inner products on
 63 $\text{SO}(3)$ and \mathbb{R}^3 . The invariant density on $\text{SE}(3)$ is chosen as $p_T \propto \mathcal{U}^{\text{SO}(3)}(r)\mathcal{N}(x)$.

64 The Stein score $\nabla \log p_t$ itself is intractable and is therefore approximated with a score network s_θ
 65 which is trained with a denoising score matching loss given by

$$\mathcal{L}_{\text{DSM}}(\theta) = \mathbb{E}[\lambda_t \|\nabla \log p_{t|0}(\mathbf{X}_t | \mathbf{X}_0) - s_\theta(t, \mathbf{X}_t)\|^2], \quad (4)$$

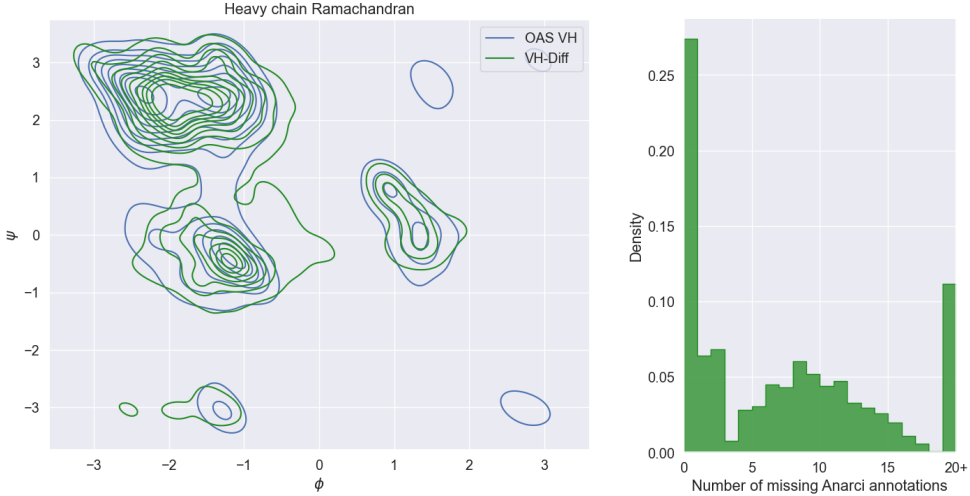


Figure 2: Left: Ramachandran plot of the dihedral angle distribution comparing the heavy chain residues from the predicted structures of the Observed Antibody Space to *VH-Diff*. Right: Distribution of number of residues that are missing annotations with Anarci, an antibody numbering tool.

66 where λ_t is a weighting schedule, $p_{t|0}$ is the density of \mathbf{X}_t given \mathbf{X}_0 , and the expectation is taken
 67 over t and the distribution of $(\mathbf{X}_0, \mathbf{X}_t)$. The loss on $SE(3)$ is decomposed into its translation and
 68 rotation components as $\mathcal{L}_{DSM} = \mathcal{L}_{DSM}^x + \mathcal{L}_{DSM}^r$.

69 To mitigate chain breaks or steric clashes and to learn the torsion angle ψ , two auxiliary losses are
 70 used. The first one is a direct mean squared error on the backbone positions \mathcal{L}_{bb} , while the second
 71 one is a local neighbourhood loss on pairwise atomic distances \mathcal{L}_{2D} . These losses are applied with a
 72 weight w when sampling t near 0, when fine-grained characteristics of the protein backbone emerge,
 73 such that the full training loss is expressed as

$$\mathcal{L} = \mathcal{L}_{DSM} + w \Theta\left(\frac{T}{4} - t\right) (\mathcal{L}_{bb} + \mathcal{L}_{2D}). \quad (5)$$

74 The score network is based on the structure module of AlphaFold2 [Jumper et al., 2021] and performs
 75 iterative updates over L layers by combining spatial and sequence based attention modules using an
 76 Invariant Point Attention and a Transformer [Vaswani et al., 2017], considering a fully connected
 77 graph structure. As well as a denoised frame, the network also predicts the torsion angle ψ for each
 78 residue, from which the positions of the backbone oxygen atoms can be reconstructed.

79 Sampling is achieved through an Euler-Maruyama discretisation of equation (3) which is approxi-
 80 mated with a geodesic random walk [Jørgensen, 1975]. To avoid destabilisation of the backbone
 81 in the final sampling steps, trajectories are instead truncated at a time $\epsilon > 0$. For all numerical
 82 applications, we use identical parameters to the original *FrameDiff* model [Yim et al., 2023].

83 3 Generating *de novo* heavy chains

84 We train this $SE(3)$ diffusion model on antibody data, specifically targeting the variable domain of
 85 the heavy chain which is more diverse and whose CDR loops play a key role in defining the binding
 86 properties of the antibody. Our dataset consists of 148,832 variable regions from the Observed
 87 Antibody Space (OAS) [Kovaltsuk et al., 2018, Olsen et al., 2022], a database of paired and unpaired
 88 antibody sequences, for which structures were predicted with ABodyBuilder2 [Abanades et al.,
 89 2022, Abanades, 2022], an antibody structure prediction model based on the structure module of
 90 AlphaFold-Multimer [Evans et al., 2022].

91 We filter our antibody dataset to retain only the heavy chain structures, and train our model, *VH-Diff*,
 92 on this single domain data. The model is obtained by fine-tuning the original *FrameDiff* weights for
 93 6 days on 8 NVIDIA A10G GPUs, using an Adam optimizer [Kingma and Ba, 2017] with a learning
 94 rate of 10^{-4} and a batch size of 64.

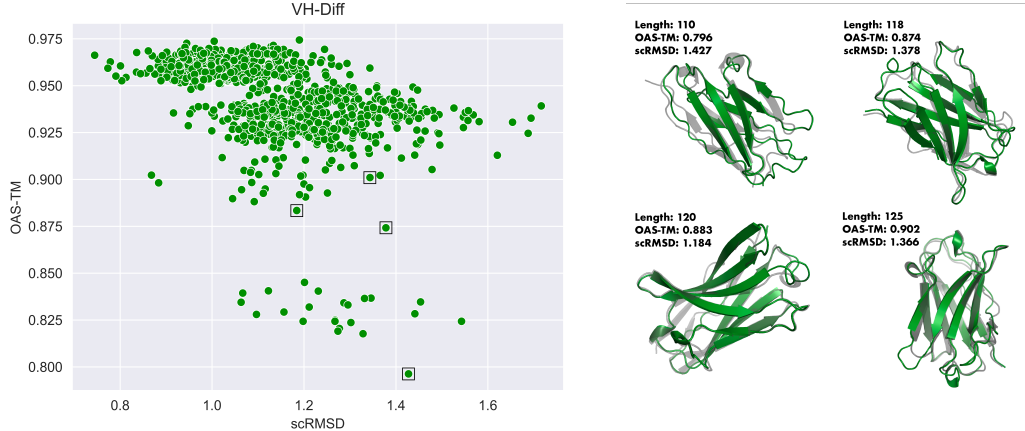


Figure 3: Left: Designability (scRMSD) vs. novelty (OAS-TM) scatter plot for *VH-Diff*. Lower values indicate higher designability and novelty. Right: Selected heavy chain samples with novel and designable structures, shown superimposed to their closest match from the Observed Antibody Space.

95 Using our trained heavy chain model, we generate unpaired heavy chain variable regions by sam-
 96 pling uniformly backbones with 110 to 130 residues. Using the `biobb_structure_checking`
 97 package [Andrio et al., 2019], we identify and remove structures that contain chain breaks, which
 98 make up 16.2% of the model output.

99 Sequences are predicted using the antibody-specific inverse folding model AbMPNN [Dreyer et al.,
 100 2023], an adaptation of the general protein model ProteinMPNN [Dauparas et al., 2022]. We sample
 101 5 sequences for each generated structure.

102 4 Study of generated structures

103 We investigated the quality of the structures generated by our *VH-Diff* model. In figure 2, we show the
 104 Ramachandran plot of the backbone dihedral (ϕ, ψ) angles, and compare it with the distributions of
 105 the corresponding structures of the OAS data, finding good overlap. We also annotate the sequences
 106 predicted with AbMPNN using Anarci [Dunbar and Deane, 2015], an antibody sequence numbering
 107 tool. We find that 88.9% of heavy chains are parsed correctly by Anarci, though some sequences
 108 have missing annotations towards their extremities. For further analysis, we remove heavy chain
 109 samples for which any of the AbMPNN predicted sequences have five or more residues which are
 110 missing anarci annotations, leaving 52.8% of the generated structures.

111 To study the designability of our models, we consider a self-consistency root mean squared error
 112 (scRMSD) metric, computing the RMSD between the C_α coordinates of our generated structures
 113 and those of the structures predicted from the AbMPNN sequences using ESMFold [Lin et al.,
 114 2022]. Specifically, we predict an ESMFold structure for all five AbMPNN sequences and keep
 115 the smallest scRMSD per sample. As a measure of novelty, we compute the maximum template
 116 modeling score [Zhang and Skolnick, 2004] between our generated samples and all structures in the
 117 OAS data (OAS-TM). A scatter plot of this designability versus novelty measure is shown in figure 3,
 118 along with selected examples that have high novelty and designability scores.

119 We compare our *VH-Diff* model with IgLM [Shuai et al., 2022], a generative antibody language
 120 model. To this end, we generate unconditioned human heavy chain sequences with IgLM, and predict
 121 their respective structures using ESMFold. The distribution of backbone dihedral angles is shown in
 122 figure 4 (left), overlaid with the corresponding OAS distribution. Here we observe a relatively good
 123 overlap with the underlying OAS distribution, though some notably discrepancies when comparing
 124 with figure 2 that indicate both models are converging to somewhat different antibody representations.
 125 We note here that while the *VH-Diff* and IgLM distributions look relatively comparable, our model
 126 was trained on a relatively small dataset of paired OAS structures, while IgLM used a training set
 127 of 558M, and that we sample uniform heavy chain lengths. On the right-hand side of figure 4, we

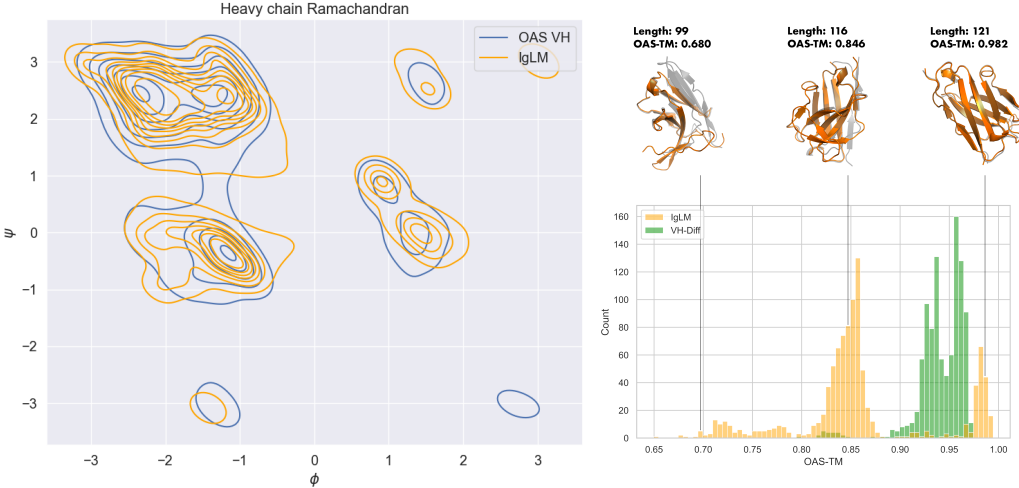


Figure 4: Left: Ramachandran plot of the dihedral angle distribution comparing the heavy chain residues from the predicted structures of the Observed Antibody Space to ESMFold predictions of IgLM heavy chain sequences. Right: Comparison of the OAS-TM distributions, along with selected IgLM structures, shown superimposed to their closest match from the Observed Antibody Space.

128 compare the distribution of OAS-TM scores for *VH-Diff* and IgLM. Here we observe that while
 129 IgLM has a few high-scoring samples that almost exactly reproduce an OAS sample, the bulk of the
 130 distribution has relatively low scores. These tend to involve large modifications in the framework
 131 regions of the heavy chain, and are therefore unlikely to be viable as antibody domains.

132 5 Conclusions

133 In this article, we have introduced a model for *de novo* heavy chain generation, *VH-Diff*. This model
 134 is derived from the recent SE(3) diffusion framework *FrameDiff*, by fine-tuning on antibody variable
 135 domains. The weights of our *VH-Diff* model are made publicly available.

136 We show that our heavy chain model is able to recapitulate the expected backbone dihedral distribution,
 137 and studied the validity of the sequences recovered from generated samples using an antibody-specific
 138 inverse folding model. Studying the designability of the generated structures by comparing them
 139 with structure predictions based on the corresponding sequences, we found excellent agreement. We
 140 probed our model for novelty by finding the closest match in the training data for each sampled
 141 structure and found it could generate structures distinct from those in the training set. Comparing
 142 *VH-Diff* with a generative language model for which structures were predicted, we found that our
 143 structure-based diffusion model had an improved coverage of the underlying dihedral distribution
 144 and novel structures that more consistently preserved conserved framework regions of the antibody.

145 Diffusion models trained on antibodies offer a promising approach to accelerate drug design through
 146 data-driven generative AI. The work presented here provides a promising step towards *de novo*
 147 antibody design. Conditioning the generation of samples to express desired properties and conserved
 148 framework residues, as well as to target specified antigens, will be key steps towards facilitating their
 149 application in therapeutic development.

150 References

- 151 Brennan Abanades. ImmuneBuilder: Deep-Learning models for predicting the structures of immune
 152 proteins., November 2022. URL <https://doi.org/10.5281/zenodo.7258553>.
- 153 Brennan Abanades, Wing Ki Wong, Fergus Boyles, Guy Georges, Alexander Bujotzek, and Char-
 154 lotte M. Deane. Immunebuilder: Deep-learning models for predicting the structures of immune
 155 proteins. *bioRxiv*, 2022. doi: 10.1101/2022.11.04.514231. URL <https://www.biorxiv.org/content/early/2022/11/04/2022.11.04.514231>.

- 157 Rebecca F. Alford, Andrew Leaver-Fay, Jeliazko R. Jeliazkov, Matthew J. O’Meara, Frank P. DiMaio,
158 Hahnbeom Park, Maxim V. Shapovalov, P. Douglas Renfrew, Vikram K. Mulligan, Kalli Kappel,
159 Jason W. Labonte, Michael S. Pacella, Richard Bonneau, Philip Bradley, Roland L. Dunbrack,
160 Rhiju Das, David Baker, Brian Kuhlman, Tanja Kortemme, and Jeffrey J. Gray. The rosetta
161 all-atom energy function for macromolecular modeling and design. *Journal of Chemical Theory
and Computation*, 13(6):3031–3048, June 2017. ISSN 1549-9618. doi: 10.1021/acs.jctc.7b00125.
- 163 Pau Andrio, Adam Hospital, Javier Conejero, Luis Jordá, Marc Del Pino, Laia Codo, Stian Soiland-
164 Reyes, Carole Goble, Daniele Lezzi, Rosa M. Badia, Modesto Orozco, and Josep Ll. Gelpí.
165 Bioexcel building blocks, a software library for interoperable biomolecular simulation workflows.
166 *Scientific Data*, 6(1):169, 2019. doi: 10.1038/s41597-019-0177-4. URL <https://doi.org/10.1038/s41597-019-0177-4>.
- 168 Valentin De Bortoli, Emile Mathieu, Michael Hutchinson, James Thornton, Yee Why Teh, and
169 Arnaud Doucet. Riemannian score-based generative modelling, 2022.
- 170 Mark L Chiu, Dennis R Goulet, Alexey Teplyakov, and Gary L Gilliland. Antibody structure and
171 function: the basis for engineering therapeutics. *Antibodies*, 8(4):55, 2019.
- 172 Alexander E. Chu, Lucy Cheng, Gina El Nesc, Minkai Xu, and Po-Ssu Huang. An all-atom protein
173 generative model. *bioRxiv*, 2023. doi: 10.1101/2023.05.24.542194. URL <https://www.biorxiv.org/content/early/2023/05/25/2023.05.24.542194>.
- 175 J. Dauparas, I. Anishchenko, N. Bennett, H. Bai, R. J. Ragotte, L. F. Milles, B. I. M. Wicky, A. Courbet,
176 R. J. de Haas, N. Bethel, P. J. Y. Leung, T. F. Huddy, S. Pellock, D. Tischer, F. Chan, B. Koepnick,
177 H. Nguyen, A. Kang, B. Sankaran, A. K. Bera, N. P. King, and D. Baker. Robust deep learning
178 based protein sequence design using proteinmpnn. *bioRxiv*, 2022. doi: 10.1101/2022.06.03.494563.
179 URL <https://www.biorxiv.org/content/early/2022/06/04/2022.06.03.494563>.
- 180 Frédéric A. Dreyer, Daniel Cutting, Constantin Schneider, Henry Kenlay, and Charlotte M. Deane.
181 Inverse folding for antibody sequence design using deep learning. In *2023 ICML Workshop
on Computational Biology*, 2023. URL https://icml-compbio.github.io/2023/papers/WCBICML2023_paper61.pdf.
- 184 James Dunbar and Charlotte M. Deane. ANARCI: antigen receptor numbering and receptor classifi-
185 cation. *Bioinformatics*, 32(2):298–300, 09 2015. ISSN 1367-4803. doi: 10.1093/bioinformatics/btv552. URL <https://doi.org/10.1093/bioinformatics/btv552>.
- 187 R. A. Engh and R. Huber. *Structure quality and target parameters*, chapter 18.3, pages 474–
188 484. John Wiley & Sons, Ltd, 2012. ISBN 9780470685754. doi: <https://doi.org/10.1107/97809553602060000857>. URL <https://onlinelibrary.wiley.com/doi/abs/10.1107/97809553602060000857>.
- 191 Richard Evans, Michael O’Neill, Alexander Pritzel, Natasha Antropova, Andrew Senior, Tim Green,
192 Augustin Žídek, Russ Bates, Sam Blackwell, Jason Yim, Olaf Ronneberger, Sebastian Bodenstein,
193 Michal Zielinski, Alex Bridgland, Anna Potapenko, Andrew Cowie, Kathryn Tunyasuvunakool,
194 Rishabh Jain, Ellen Clancy, Pushmeet Kohli, John Jumper, and Demis Hassabis. Protein complex
195 prediction with alphafold-multimer. *bioRxiv*, 2022. doi: 10.1101/2021.10.04.463034. URL
196 <https://www.biorxiv.org/content/early/2022/03/10/2021.10.04.463034>.
- 197 Jonathan Ho, Ajay Jain, and Pieter Abbeel. Denoising diffusion probabilistic models, 2020.
- 198 Erik Jørgensen. The central limit problem for geodesic random walks. *Zeitschrift für Wahrscheinlichkeitstheorie und Verwandte Gebiete*, 32(1):1–64, 1975. doi: 10.1007/BF00533088. URL
199 <https://doi.org/10.1007/BF00533088>.
- 201 John Jumper, Richard Evans, Alexander Pritzel, Tim Green, Michael Figurnov, Olaf Ronneberger,
202 Kathryn Tunyasuvunakool, Russ Bates, Augustin Žídek, Anna Potapenko, Alex Bridgland,
203 Clemens Meyer, Simon A. A. Kohl, Andrew J. Ballard, Andrew Cowie, Bernardino Romera-
204 Paredes, Stanislav Nikolov, Rishabh Jain, Jonas Adler, Trevor Back, Stig Petersen, David Reiman,
205 Ellen Clancy, Michal Zielinski, Martin Steinegger, Michalina Pacholska, Tamas Berghammer,
206 Sebastian Bodenstein, David Silver, Oriol Vinyals, Andrew W. Senior, Koray Kavukcuoglu,

- 207 Pushmeet Kohli, and Demis Hassabis. Highly accurate protein structure prediction with
208 alphafold. *Nature*, 596(7873):583–589, 2021. doi: 10.1038/s41586-021-03819-2. URL
209 <https://doi.org/10.1038/s41586-021-03819-2>.
- 210 Diederik P. Kingma and Jimmy Ba. Adam: A method for stochastic optimization, 2017.
- 211 Aleksandr Kovaltsuk, Jinwoo Leem, Sebastian Kelm, James Snowden, Charlotte M. Deane, and
212 Konrad Krawczyk. Observed Antibody Space: A Resource for Data Mining Next-Generation Se-
213 quencing of Antibody Repertoires. *The Journal of Immunology*, 201(8):2502–2509, 10 2018. ISSN
214 0022-1767. doi: 10.4049/jimmunol.1800708. URL <https://doi.org/10.4049/jimmunol.1800708>.
- 216 Yeqing Lin and Mohammed AlQuraishi. Generating novel, designable, and diverse protein structures
217 by equivariantly diffusing oriented residue clouds, 2023.
- 218 Zeming Lin, Halil Akin, Roshan Rao, Brian Hie, Zhongkai Zhu, Wenting Lu, Allan dos Santos Costa,
219 Maryam Fazel-Zarandi, Tom Sercu, Sal Candido, and Alexander Rives. Language models of
220 protein sequences at the scale of evolution enable accurate structure prediction. *bioRxiv*, 2022.
221 doi: 10.1101/2022.07.20.500902. URL <https://www.biorxiv.org/content/early/2022/07/21/2022.07.20.500902>.
- 223 Karolis Martinkus, Jan Ludwiczak, Kyunghyun Cho, Wei-Ching Liang, Julien Lafrance-Vanassee,
224 Isidro Hotzel, Arvind Rajpal, Yan Wu, Richard Bonneau, Vladimir Gligorjevic, and Andreas
225 Loukas. Abdifuser: Full-atom generation of in-vitro functioning antibodies, 2023.
- 226 Jo Erika Narciso, Iris Uy, April Cabang, Jenina Chavez, Juan Pablo, Gisela Padilla-Concepcion, and
227 Eduardo Padlan. Analysis of the antibody structure based on high-resolution crystallographic
228 studies. *New biotechnology*, 28:435–47, 04 2011. doi: 10.1016/j.nbt.2011.03.012.
- 229 Tobias H. Olsen, Fergus Boyles, and Charlotte M. Deane. Observed antibody space: A di-
230 verse database of cleaned, annotated, and translated unpaired and paired antibody sequences.
231 *Protein Science*, 31(1):141–146, 2022. doi: <https://doi.org/10.1002/pro.4205>. URL <https://onlinelibrary.wiley.com/doi/abs/10.1002/pro.4205>.
- 233 Richard W. Shuai, Jeffrey A. Ruffolo, and Jeffrey J. Gray. Generative language modeling for antibody
234 design. *bioRxiv*, 2022. doi: 10.1101/2021.12.13.472419. URL <https://www.biorxiv.org/>
235 content/early/2022/12/20/2021.12.13.472419.
- 236 Yang Song, Jascha Sohl-Dickstein, Diederik P. Kingma, Abhishek Kumar, Stefano Ermon, and Ben
237 Poole. Score-based generative modeling through stochastic differential equations, 2021.
- 238 Yuko Tsuchiya and Kenji Mizuguchi. The diversity of h3 loops determines the antigen-binding
239 tendencies of antibody cdr loops. *Protein science : a publication of the Protein Society*, 25, 01
240 2016. doi: 10.1002/pro.2874.
- 241 Ashish Vaswani, Noam Shazeer, Niki Parmar, Jakob Uszkoreit, Llion Jones, Aidan N. Gomez, Lukasz
242 Kaiser, and Illia Polosukhin. Attention is all you need, 2017.
- 243 Joseph L. Watson, David Juergens, Nathaniel R. Bennett, Brian L. Trippe, Jason Yim, Helen E.
244 Eisenach, Woody Ahern, Andrew J. Borst, Robert J. Ragotte, Lukas F. Milles, Basile I. M.
245 Wicky, Nikita Hanikel, Samuel J. Pellock, Alexis Courbet, William Sheffler, Jue Wang, Preetham
246 Venkatesh, Isaac Sappington, Susana Vázquez Torres, Anna Lauko, Valentin De Bortoli, Emile
247 Mathieu, Regina Barzilay, Tommi S. Jaakkola, Frank DiMaio, Minkyung Baek, and David Baker.
248 Broadly applicable and accurate protein design by integrating structure prediction networks and
249 diffusion generative models. *bioRxiv*, 2022. doi: 10.1101/2022.12.09.519842. URL <https://www.biorxiv.org/content/early/2022/12/10/2022.12.09.519842>.
- 251 Zachary Wu, Kadina E. Johnston, Frances H. Arnold, and Kevin K. Yang. Protein sequence design
252 with deep generative models. *Current Opinion in Chemical Biology*, 65:18–27, 2021. ISSN 1367-
253 5931. doi: <https://doi.org/10.1016/j.cbpa.2021.04.004>. URL <https://www.sciencedirect.com/science/article/pii/S136759312100051X>. Mechanistic Biology * Machine Learning
254 in Chemical Biology.

256 Jason Yim, Brian L Trippe, Valentin De Bortoli, Emile Mathieu, Arnaud Doucet, Regina Barzilay,
257 and Tommi Jaakkola. Se(3) diffusion model with application to protein backbone generation. *arXiv*
258 *preprint arXiv:2302.02277*, 2023.

259 Yang Zhang and Jeffrey Skolnick. Scoring function for automated assessment of protein structure
260 template quality. *Proteins*, 57(4):702—710, December 2004. ISSN 0887-3585. doi: 10.1002/prot.
261 20264. URL <https://doi.org/10.1002/prot.20264>.